J. Fluid Mech. (2003), *vol.* 478, *pp.* 1–10. © 2003 Cambridge University Press
DOI: 10.1017/S0022112002002616 Printed in the United Kingdom

Evolution of a narrow-band spectrum of random surface gravity waves

By KRISTIAN B. DYSTHE[1], KARSTEN TRULSEN[2]†, HARALD E. KROGSTAD[3] AND HERVÉ SOCQUET-JUGLARD[1]

[1]Department of Mathematics, University of Bergen, Johs. Brunsgt. 12, N-5008 Bergen, Norway
[2]SINTEF Applied Mathematics, P.O. Box 124 Blindern, N-0314 Oslo, Norway
[3]Department of Mathematical Sciences, NTNU, N-7491 Trondheim, Norway

(Received 10 April 2002 and in revised form 27 August 2002)

Numerical simulations of the evolution of gravity wave spectra of fairly narrow bandwidth have been performed both for two and three dimensions. Simulations using the nonlinear Schrödinger (NLS) equation approximately verify the stability criteria of Alber (1978) in the two-dimensional but not in the three-dimensional case. Using a modified NLS equation (Trulsen *et al.* 2000) the spectra 'relax' towards a quasi-stationary state on a timescale $(\epsilon^2\omega_0)^{-1}$. In this state the low-frequency face is steepened and the spectral peak is downshifted. The three-dimensional simulations show a power-law behaviour ω^{-4} on the high-frequency side of the (angularly integrated) spectrum.

1. Introduction

It is well-known that a uniform train of surface gravity waves is unstable to the so-called modulational instability or Benjamin–Feir (BF) instability (Lighthill 1965, 1967; Whitham 1967; Benjamin & Feir 1967; Zakharov 1968).

The stability of nearly Gaussian random wave fields of narrow bandwidth was considered by Alber & Saffman (1978), Alber (1978) and Crawford, Saffman & Yuen (1980). For waves on deep water they found that the modulational instability occurs provided that the relative spectral width, σ, is less than twice the average steepness, $\epsilon \equiv k_0\bar{a}$, where k_0 is the central wavenumber, and $\bar{a} = (2\overline{\eta^2})^{1/2}$ is the r.m.s. value of the amplitude.

For deep water waves the results of Alber & Saffman (1978) and Alber (1978) are based on the nonlinear Schrödinger (NLS) equation, which is the lowest-order model equation in the relative spectral width and wave steepness that takes into account both dispersion and nonlinearity. It can be written

$$\mathrm{i}\left(\frac{\partial B}{\partial t} + v_g\frac{\partial B}{\partial x}\right) + \frac{1}{2}\left(\frac{\mathrm{d}v_g}{\mathrm{d}k}\frac{\partial^2 B}{\partial x^2} + \frac{v_g}{k_0}\frac{\partial^2 B}{\partial y^2}\right) - \frac{\omega_0 k_0^2}{2}|B|^2 B = 0, \tag{1}$$

where the surface elevation η is given by

$$\eta = \tfrac{1}{2}\left(B\mathrm{e}^{\mathrm{i}(k_0x-\omega_0t)} + B_2\mathrm{e}^{2\mathrm{i}(k_0x-\omega_0t)} + \cdots + \text{c.c.}\right) \tag{2}$$

where B and B_2 are slowly varying functions of $\boldsymbol{x} = (x, y)$ and t.

† Current address: Department of Mathematics, University of Oslo, P.O. Box 1053 Blindern, N-0316 Oslo, Norway.

Alber (1978) considers the case where B is a slowly varying, nearly Gaussian random function of $\boldsymbol{x}$ and t. He develops a nonlinear transport equation for the ensemble-averaged envelope spectrum $F(\boldsymbol{K}, \boldsymbol{x}, t)$ (where $\int F \mathrm{d}\boldsymbol{K} = 2\overline{\eta^2} = \overline{a^2}$) centred around $\boldsymbol{k}_0 = (k_0, 0)$, where the wave vector is $\boldsymbol{k} = \boldsymbol{k}_0 + k_0\boldsymbol{K}$ and $\boldsymbol{K} = (K_x, K_y)$. The stability of a random homogeneous and stationary wave field with spectrum $F_0(\boldsymbol{K})$ is then investigated, where $F_0(\boldsymbol{K})$ is taken to have the Gaussian shape

$$F_0(\boldsymbol{K}) = \frac{\overline{\eta^2}}{\pi\sigma_x\sigma_y} \exp\left[\frac{1}{2}\left(-\frac{K_x^2}{\sigma_x^2} - \frac{K_y^2}{\sigma_y^2}\right)\right], \tag{3}$$

and where σ_x and σ_y are the relative bandwidths in the x- and y-directions, respectively. Alber's result for three dimensions is unfortunately somewhat difficult to interpret except for the case when the spectrum is symmetric around $\boldsymbol{k}_0$ (i.e. $\sigma_x = \sigma_y \equiv \sigma$). In that case, a necessary and sufficient condition for stability is found to be

$$\sigma > 2\epsilon, \tag{4}$$

which is formally identical to the two-dimensional condition of Alber & Saffman (1978) and Alber (1978).

Crawford *et al.* (1980) extended the work of Alber. Their starting point is the so-called Zakharov integral equation, which does not have any spectral limitations. They derive the corresponding transport equation governing the evolution of a non-homogeneous random wave field, assuming the zero-fourth-order cumulant hypotheses. By further taking the narrow-band limit, i.e. evaluating the coupling coefficients in their integro-differential equation at the central wave vector, they arrive at the same transport equation as Alber. To investigate the stability of narrow-band random wavetrains, they choose a different initial spectrum, namely

$$F_0(\boldsymbol{K}) = \frac{2\overline{\eta^2}\sigma_x\sigma_y}{\pi^2\left(K_x^2 + \sigma_x^2\right)\left(K_y^2 + \sigma_y^2\right)}, \tag{5}$$

where σ_x and σ_y are the 'half-widths' in the x- and y-directions, respectively. They find that the spectrum in (5) is stable provided that

$$\sigma_x > 2\epsilon. \tag{6}$$

For the symmetric case $\sigma_x = \sigma_y$, the condition (6) is formally the same as Alber's condition (4) although the definitions of the σ, as well as the shape of the spectra, are quite different. Note also that the relative spectral width transversal to the main wave direction, σ_y, does not enter the condition (6).

These results suggest that narrow-band spectra do not change on the timescale $(\epsilon^2\omega_0)^{-1}$, which is the typical timescale for the BF instability and henceforth referred to as the BF timescale, provided that the relative spectral width exceeds a certain threshold. If this is the case, the spectral change should only occur on the much longer timescale $(\epsilon^4\omega_0)^{-1}$, i.e. the Hasselmann timescale (Hasselmann 1962; Crawford *et al.* 1980).

To our knowledge these important results, though more than 20 years old, have not been compared to experiments or numerical simulations.

Previous simulations using the NLS equation have to some extent concentrated on the stability of Stokes waves, or the evolution of a few Fourier modes. Here the phenomena of recurrence or near recurrence appear, as thoroughly discussed by Yuen & Ferguson (1978) for the two-dimensional case. As the number of Fourier modes

increases (although they may be very small initially – see Trulsen & Dysthe 1997), the recurrence phenomenon disappears from the computational time horizon. In the three-dimensional simulations to be presented here with more than 10^4 modes, the probability of seeing a near recurrence becomes vanishingly small.

In the present paper we report numerical simulations on the evolution of narrow-band spectra in two and three dimensions with four different numerical models:

(i) the NLS equation (1);

(ii) the modified nonlinear Schrödinger (MNLS) equation of Dysthe (1979) which includes terms to the next order in nonlinearity and bandwidth, assuming the relative spectral width to be of order ϵ;

(iii) the broader bandwidth equation of Trulsen & Dysthe (1996) which relaxes the bandwidth in the MNLS equation to be of order $\epsilon^{1/2}$;

(iv) the equation of Trulsen *et al.* (2000) which extends the MNLS equation with exact linear dispersion.

For the present applications we have found that the two extensions (iii) and (iv) of the MNLS equation give practically the same results as the MNLS equation, (ii), for the behaviour near the spectral peak, hence these results will collectively be referred to as MNLS in the following. The MNLS has been compared with wave tank experiments (Trulsen & Stansberg 2001) and shown to give excellent agreement up to times one order of magnitude larger than the BF timescale.

The two-dimensional results using the NLS equation only approximately confirm the stability conditions of Alber & Saffman (1978) and Alber (1978). They also show that an unstable spectrum relaxes, on the timescale of the BF instability, to a wider symmetrical spectrum that appears to be stable within the time horizon for the equation.

The three-dimensional NLS simulations, however, do not agree with the theoretical predictions. The initial spectral distributions spread out in both horizontal directions, regardless of whether they satisfy the Alber stability criterion or not. Also, for the three-dimensional case, the spectral evolution takes place on the BF timescale.

The MNLS simulations, on the other hand, show a somewhat different evolution both in two and three dimensions. Regardless of the initial spectral width, the spectra evolve on the BF timescale from an initial symmetrical form into a skewed shape with a downshift of the peak frequency. In three dimensions, the angularly integrated spectrum shows an evolution towards a power-law behaviour ω^{-4} on the high-frequency side.

2. The numerical simulations

The NLS equation is given in (1), while the higher-order equations can be found in Dysthe (1979), Trulsen & Dysthe (1996) and Trulsen *et al.* (2000), and are not reproduced here. Length and time are normalized with the characteristic wavenumber and frequency, k_0 and $\omega_0 = \sqrt{gk_0}$, respectively.

We use the numerical method described by Lo & Mei (1985, 1987) with periodic boundary conditions in both horizontal directions. A uniform grid in the physical and wave vector planes with $N_x = N_y = 128$ points is employed. With a computational domain of 50 characteristic wavelengths in each horizontal direction, we set the discretization of the wave vector plane to be $\Delta K_x = \Delta K_y = 1/50$. However, we only employ the modes with relative bandwidth less than unity, $|\boldsymbol{K}| < 1$. The physical plane has dimensions $L_x = 2\pi/\Delta K_x$ and $L_y = 2\pi/\Delta K_y$, and has the grid points $x_j = L_x j/N_x$, $j = 0, 1, \ldots, N_x - 1$ and $y_l = L_y l/N_y$, $l = 0, 1, \ldots, N_y - 1$.

In all simulations we start with the initial Gaussian bell-shaped spectrum (3) with $\sigma_x = \sigma_y = \sigma$, or the corresponding one-dimensional form.

Note that in the three-dimensional simulations the spectrum has a small angular spread around the main wave direction, with a half-angle spread $\theta \simeq \sigma$ (approximately 6° and 12° for $\sigma = 0.1$ and 0.2, respectively).

For each sample simulation the Fourier components are initialized with random phases and a modulus proportional to the square root of the spectrum

$$\hat{B}_{mn}(0) = \epsilon \sqrt{\frac{\Delta K_x \Delta K_y}{2\pi\sigma^2}} \exp\left(-\frac{(m\Delta K_x)^2 + (n\Delta K_y)^2}{4\sigma^2}\right) \exp \mathrm{i}\theta_{mn}, \tag{7}$$

where the random variables θ_{mn} are uniformly distributed on the interval $[0, 2\pi)$. The physical amplitude B is obtained through the discrete Fourier transform

$$B(x_j, y_l, t) = \sum_{m,n} \hat{B}_{mn}(t) \exp(\mathrm{i}(m\Delta K_x x_j + n\Delta K_y y_l)). \tag{8}$$

In order to have a truly Gaussian initial condition, each Fourier coefficient should be chosen as an independent complex Gaussian variable with a variance proportional to the corresponding value of the spectrum. However, numerical experiments using complex Gaussian Fourier coefficients, unlike when using a uniformly distributed phase only, yielded virtually identical time evolutions of the spectrum.

The spectra shown below are obtained as the squared modulus of the Fourier coefficients and, in addition, are ensemble averaged and smoothed. In the two-dimensional simulations an ensemble of 50 independent simulations has been used, whereas for the three-dimensional simulations only 20 are used due to the long CPU-time involved. The averaged wavenumber spectra from the three-dimensional simulations have therefore been smoothed with a moving average Gaussian bell with standard deviation $1.7\Delta K_x$.

In the simulations presented here we have taken the average steepness ϵ to be 0.1. We have performed simulations with other values of the steepness and the results were quite similar. In particular, the relevant timescale for the spectral evolution was still found to be the BF scale, $(\epsilon^2\omega_0)^{-1}$.

Our computations conserve the total energy and momentum within the bandwidth constraint with high accuracy. We do not account for coupling with free-wave Fourier modes outside the bandwidth constraint.

In Trulsen & Stansberg (2001) quantitative comparisons were made between simulations and wave tank experiments of long-crested bichromatic waves. It was found that while the NLS equation gave good quantitative comparisons with the experiments up to $x \approx (\epsilon^2 k_0)^{-1}$, the corresponding range for the MNLS equation was $x \approx 5(\epsilon^2 k_0)^{-1}$. Translated to temporal, rather than spatial evolution, these numbers are $t \approx 2(\epsilon^2\omega_0)^{-1}$ and $t \approx 10(\epsilon^2\omega_0)^{-1}$, respectively. This suggests that the NLS equation can be reliably used up to the BF scale, while the MNLS equation can be reliably used an order of magnitude longer. We have taken the present MNLS simulations up to a maximum time $t = 10(\epsilon^2\omega_0)^{-1}$, which should be in the domain in which the equations are reliable.

2.1. *Two-dimensional simulations*

In the NLS simulations the Alber criterion $\sigma > 2\epsilon$ for suppression of the modulational instability is only approximately verified. Starting with the case $\sigma < 2\epsilon$, we find that the spectrum broadens symmetrically until it reaches a quasi steady width. This

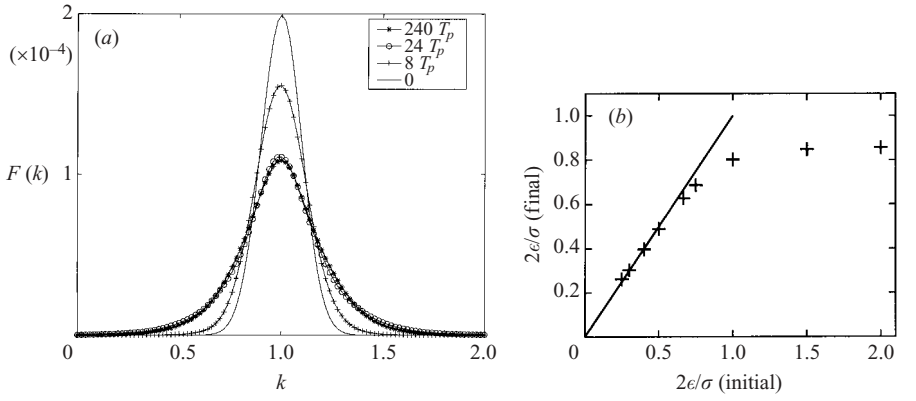

FIGURE 1. Spectral evolution of the two-dimensional NLS equation starting with an initial Gaussian spectrum. (*a*) The spectrum at four different times with initial width $\sigma = 0.1$ and steepness $\epsilon = 0.1$. (*b*) The relation between initial and final spectral widths: —, prediction of Alber; +, numerical result. Here $\epsilon = 0.05$.

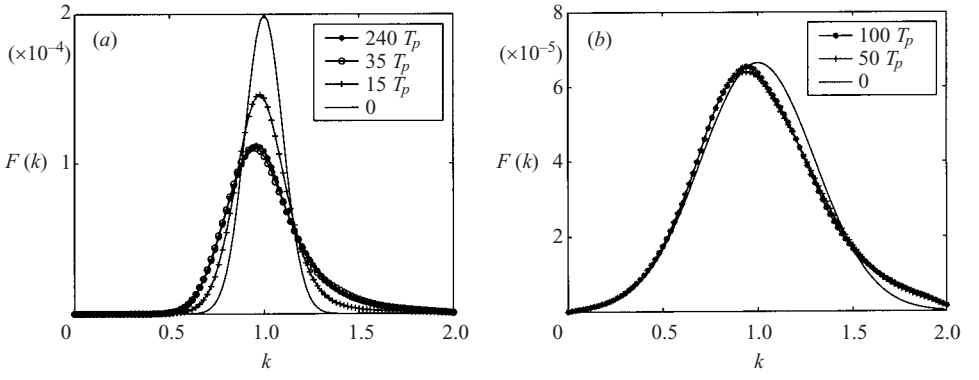

FIGURE 2. Spectral evolution of solutions of the MNLS equation. Gaussian initial spectrum with (*a*) $\sigma = 0.1$, $\epsilon = 0.1$, and (*b*) $\sigma = 0.3$, $\epsilon = 0.1$.

relaxation of the spectrum clearly takes place on the BF-timescale $(\epsilon^2\omega_0)^{-1}$. This is illustrated in figure 1(*a*), where the initial parameters are $\epsilon = 0.1$ and $\sigma = 0.1$. Even for the case $\sigma > 2\epsilon$ there is still a small widening of the spectrum. This is shown in figure 1(*b*) illustrating the relation between the final spectral width (after the relaxation to a quasi-steady state) and the initial width.† The relative spectral width is here defined as $\{\int K^2 F \, \mathrm{d}K / \int F \, \mathrm{d}K\}^{1/2}$.

In the MNLS simulations, the initially symmetric Gaussian shape of the spectrum does not persist regardless of the initial spectral width. The spectrum evolves, on the timescale $(\epsilon^2\omega_0)^{-1}$, towards a quasi-steady state which has an asymmetrical shape with a steepening of the low-frequency side and a widening of the high-frequency side and, consequently, a downshift of the spectral peak. This is shown in figure 2 for the initial widths $\sigma = 0.1$ and $\sigma = 0.3$.

† This was overlooked in the initial version of the paper, and brought to our attention by Dr P Janssen.

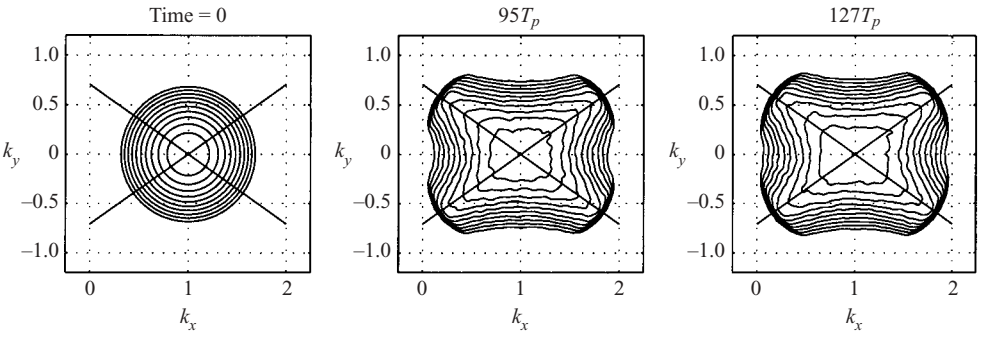

FIGURE 3. Evolution of an initially Gaussian spectrum for the three-dimensional NLS equation. The contour interval is logarithmic (2.5 dB) covering −25 dB. The cross indicates the directions of the most unstable BF modes, $K_y = \pm 2^{-1/2} K_x$.

Mori & Yasuda (2001, 2002) have found results qualitatively similar to ours. They use a numerical two-dimensional model based on the full Euler equations. Starting from a Wallops-type spectrum they show that a widening takes place if the initial width is small.

2.2. *Three-dimensional simulations*

In three dimensions the NLS simulations do not support the theoretical result of Alber (1978). A considerable widening of the spectrum is seen in all our simulations regardless of the initial spectral width σ. When $\sigma < 2\epsilon$ the spectrum flattens out almost to a plateau shape. When $\sigma \geqslant 2\epsilon$, the spectrum extends predominantly in the directions $K_y/K_x = \pm 2^{-1/2}$, coinciding with the directions for the most unstable BF modulations (see also Longuet-Higgins 1976). This is shown in figure 3 where $\sigma = 0.2$ and $\epsilon = 0.1$. For large times, we see that energy accumulates near the unit bandwidth constraint $|\boldsymbol{K}| = 1$, and eventually renders the simulation invalid. Without the bandwidth constraint, Martin & Yuen (1980) found that the NLS equation could suffer energy leakage to arbitrarily large Fourier modes along the diagonal directions.

Figure 4 shows results of similar computations carried out using the MNLS equation. The initial spectral widths are $\sigma = 0.1$ in the upper row, and $\sigma = 0.2$ in the lower row. In this case we see an asymmetric development with a downshift of the spectral peak, k_p (i.e. $k_p < k_0$) and an angular widening, mainly for $k > k_p$.

For the corresponding angularly integrated spectra shown in figure 5 some steepening is seen on the low-frequency side, $k < k_p$, while a power-law behaviour $k^{-2.5}$ (corresponding to a power law ω^{-4} for the frequency spectrum) is seen on the high-frequency side, $k > k_p$. It is also interesting to note that the level of the $k^{-2.5}$ line is apparently the same for the two cases.

3. Discussion

The original intention of this work was to verify the theoretical results of Alber (1978), that wave spectra broader than a certain threshold value (4) would not evolve on the BF timescale $(\epsilon^2 \omega_0)^{-1}$. We anticipated that these results based on the NLS equation would also be valid for the MNLS equation.

The NLS simulations only approximately verified Alber's result in two dimensions, while in three dimensions a widening of the spectra was seen regardless of the initial

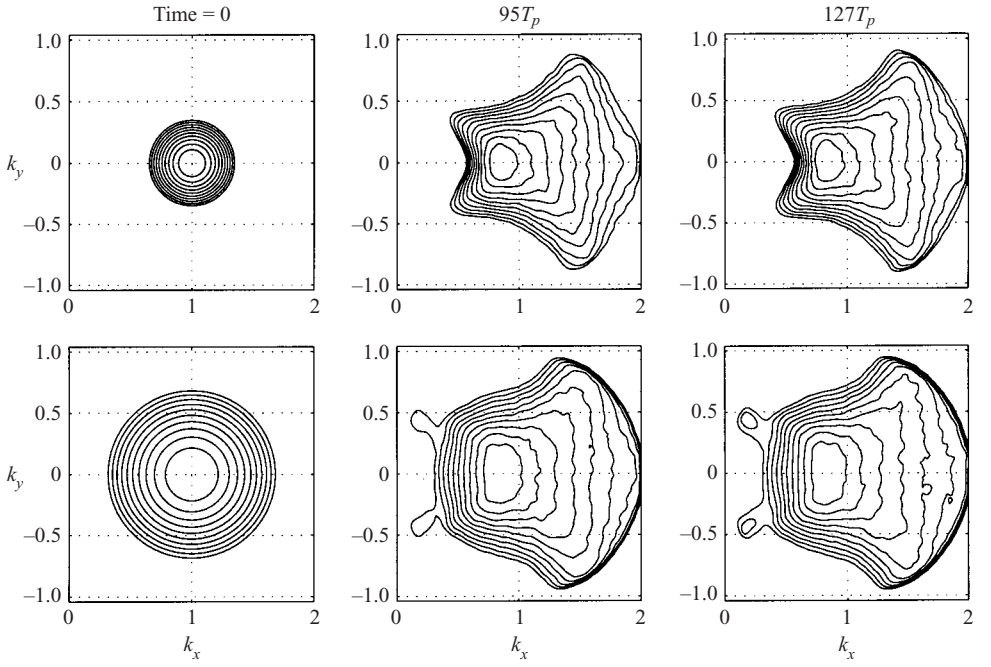

FIGURE 4. Spectral evolution with the MNLS equation. The contour interval 2.5 dB down to −25 dB. The steepness ε is equal to 0.1, and the spectral width is $\sigma = 0.1$ in the upper row, and $\sigma = 0.2$ in the lower row.

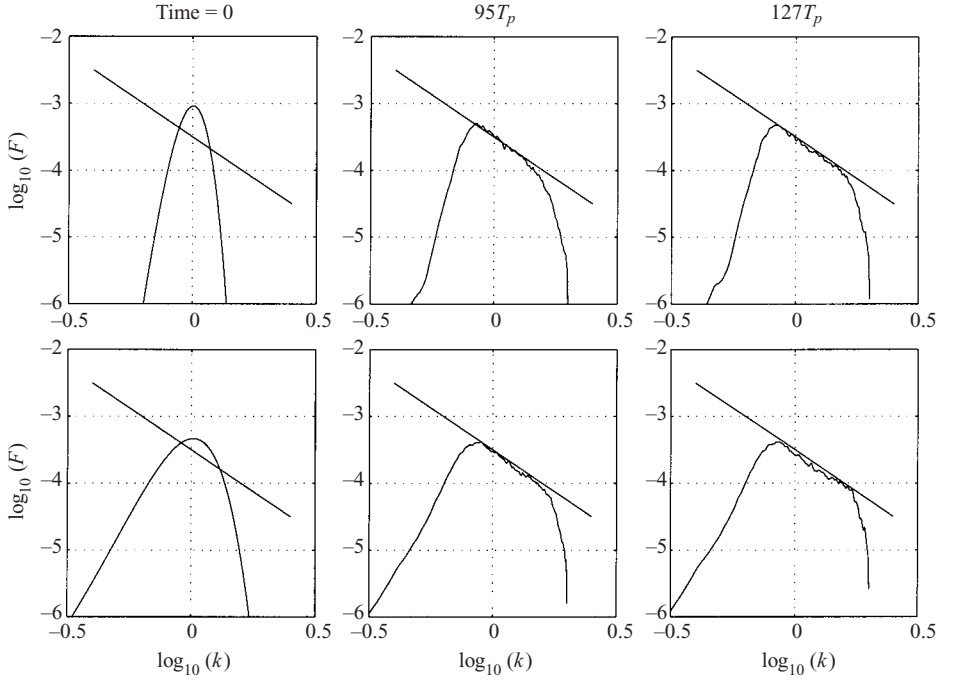

FIGURE 5. Evolution of the angularly integrated spectra corresponding to those in figure 4. The lines have slopes −2.5.

width, as explained above. The MNLS simulations were rather surprising. Regardless of the initial spectral width, the simulations show that narrow Gaussian-shaped spectra quickly evolve into a quasi-stationary state with a downshifted spectral peak. In the three-dimensional case a power-law behaviour $k^{-2.5}$ (or ω^{-4}) above the peak is observed for the angularly integrated spectrum. The relaxation takes place on the BF timescale $(\epsilon^2\omega_0)^{-1}$. This timescale is much faster than the $(\epsilon^4\omega_0)^{-1}$ timescale implied by the Hasselmann spectral evolution equation (Hasselmann 1962).

For a realistic ocean wave spectrum, the effects of wind input and dissipation by wave breaking are of course important for its evolution. For young waves these effects change the spectrum on a comparable or even faster timescale than the BF scale. Our simulations are restricted to fairly narrow spectra corresponding to a region around the spectral peak (carrying perhaps 80% or more of the total wave energy). For these waves the ratio of the e-folding time, T_e, due to wind input, to the peak period T_p depends strongly on the wave age. From a semi-empirical formula for the wind growth due to Hsiao & Shemdin (1983) we find that

$$\frac{T_e}{T_p} \simeq \frac{10^3}{(0.85(U_{10}/C_p)\cos\theta - 1)^2} \tag{9}$$

where θ is the angle between the phase velocity and the wind. Using (9) we find that $T_e/T_p > 1000$ when the wave age $C_p/U_{10} > 0.42$. For long storm waves on the open ocean T_e may thus be considerably longer than the 'relaxation' time of the order of $100T_p$ that we find. Thus, the fact that the wind input is absent in our simulations seems consistent provided that the wave age is not too small. The spectral evolution also shows realistic features like the steepening of the low-frequency part ($\omega < \omega_p$) and the power-law behaviour for the high-frequency part ($\omega > \omega_p$), with a corresponding frequency downshift. For the long-term consistent downshift of a realistic wave spectrum, however, we believe that the wind input and dissipation are essential.

After the submission of our paper, our results were presented at the WISE (Waves In Shallow-water Environments) meeting in Bergen, Norway, May 13–16, 2002. Interestingly, similar two-dimensional results were also presented by Peter Janssen (see Janssen 2002) using the NLS and the Zakharov integral equations, and by Miguel Onorato *et al.* (see Onorato *et al.* 2002) in three dimensions using the full Euler equations (they demonstrated the power-law behaviour $k^{5/2}$ to occur for a much wider spectral range than shown in the present paper). As some of the same conclusions have been reached through three independent efforts using three different model equations, we believe that these results are important and not the consequence of a particular choice of wave model.

It is not obvious how these results can be reconciled with the Hasselmann picture, however. Janssen (1983) showed that the approximation to the Hasselmann equation given by Dungey & Hui (1979) for narrow-band spectra can be derived from the MNLS equations using the same statistical assumptions as Hasselmann. It is perhaps worth noting that the zero-cumulant hypotheses implied by the approximate multivariate complex Gaussian property of the Fourier coefficients, and necessary for the derivation of Hasselmann's equation, may not be realistic in the present case. Even if the initial Fourier coefficients are chosen to be independent complex Gaussian variables, the non-linear deterministic simulation will couple the Fourier coefficients and destroy their Gaussian property. Also, the homogeneity in time and space assumed

in the Hasselmann treatment may not be realistic. The two-dimensional theoretical and simulation results by Janssen referred to above seem to indicate that the deviation from the Gaussian property is more important than non-homogeneity.

We find, by making longer simulations than those shown above, that even after the spectrum has relaxed to the new shape there is still a very slow change. It is not possible for us to decide whether this indicates an evolution as predicted by the Hasselmann equation, as the time horizon for our numerical model is too limited.

This research has been supported by the BeMatA program of the Research Council of Norway (139177/431), by Norsk Hydro, by the European Union through the EnviWave project (EVG1–CT–2001–00051) and by Statoil.

REFERENCES

Alber, I. E. 1978 The effects of randomness on the stability of two-dimensional surface wavetrains. *Proc. R. Soc. Lond.* A **363**, 525–546.

Alber, I. E. & Saffman, P. G. 1978 Stability of Random nonlinear deep water waves with finite bandwidth spectrum.*TWR Defense and Spacesystems Group Rep.* 31326-6035-RU-00.

Benjamin, T. B. & Feir, J. E. 1967 The disintegration of wave trains on deep water. Part 1. Theory. *J. Fluid Mech.* **27**, 417–430.

Crawford, D. R., Saffman, P. G. & Yuen, H. C. 1980 Evolution of a random inhomogeneous field of nonlinear deep-water gravity waves. *Wave Motion* **2**, 1–16.

Dungey, J. C. & Hui, W. H. 1979 Nonlinear energy transfer in a narrow gravity-wave spectrum. *Proc. R. Soc. Lond.* A **368**, 239–265.

Dysthe, K. B. 1979 Note on a modification to the nonlinear Schrödinger equation for application to deep water waves. *Proc. R. Soc. Lond.* A **369**, 105–114.

Hasselmann, K. 1962 On the nonlinear energy transfer in a gravity-wave spectrum. Part 1. General theory. *J. Fluid Mech.* **12**, 481–500.

Hsiao, G. C. & Shemdin, O. H. 1983 Measurements of wind velocity and pressure with a wave follower during MARSEN. *J. Geophys. Res.* **88**, 9841–9849.

Janssen, P. A. E. M. 1983 On a fourth-order envelope equation for deep-water waves. *J. Fluid Mech.* **126**, 1–11.

Janssen, P. A. E. M. 2002 Nonlinear four wave interaction and freak waves. *ECMWF Tech. Mem.*

Lighthill, M. J. 1965 Contribution to the theory of waves in nonlinear dispersive systems. *J. Inst. Maths Applics.* **1**, 269–306.

Lighthill, M. J. 1967 Some special cases treated by the Whitham theory. *Proc. R. Soc. Lond.* A **299**, 28–53.

Lo, E. & Mei, C. C. 1985 A numerical study of water-wave modulation based on a higher-order nonlinear Schrödinger equation. *J. Fluid Mech.* **150**, 395–416.

Lo, E. Y. & Mei, C. C. 1987 Slow evolution of nonlinear deep water waves in two horizontal directions: A numerical study. *Wave Motion* **9**, 245–259.

Longuet-Higgins, M. S. 1976 On the nonlinear transfer of energy in the peak of a gravity wave spectrum: a simplified model. *Proc. R. Soc. Lond.* A **347**, 311–328.

Martin, D. U. & Yuen, H. C. 1980 Quasi-recurring energy leakage in the two-space-dimensional nonlinear Schrödinger equation. *Phys. Fluids* **23**, 881–883.

Mori, D. & Yasuda, T. 2001 Effects of high-order nonlinear interactions on gravity waves. *Proc. Rogue Waves 2000* (ed. M. Olagnon & G. Athanassoulis).

Mori, D. & Yasuda, T. 2002 Effects of high-order nonlinear interactions on unidirectional wave trains. *Ocean Engng* **29**, 1233–1245.

Onorato, M., Osborne, A. R., Serio, M., Resio, D., Pushkarev, A., Zakharov, V. & Brandini, C. 2002 Freely decaying weak turbulence for sea surface waves. *Phys. Rev. Lett.* **89**(14), art. no. 144501.

Trulsen, K. & Dysthe, K. B. 1996 A modified nonlinear Schrödinger equation for broader bandwidth gravity waves on deep water. *Wave Motion* **24**, 281–289.

Trulsen, K., Kliakhandler, I., Dysthe, K. B. & Velarde, M. G. 2000 On weakly nonlinear modulation of waves on deep water. *Phys. Fluids* **10**, 2432–2437.

Trulsen, K. & Stansberg, C. T. 2001 Spatial evolution of water surface waves: Numerical simulation and experiment of bichromatic waves. In *Proc. ISOPE 2001* **3**, 71–77.

Whitham, G. B. 1967 Non-linear dispersion of water waves. *Proc. R. Soc. Lond.* A **299**, 6–25.

Yuen, H. C. & Ferguson, W. E. 1978 Relationship between Benjamin–Feir instability and recurrence in the nonlinear Schrödinger equation. *Phys. Fluids* **21**, 1275–1278.

Zakharov, V. E. 1968 Stability of periodic waves of finite amplitude on the surface of deep water. *Zh. Prikl. Mekh. Tekh. Fiz.* **9**, 86–94. (English transl. *J. Appl. Mech. Tech. Phys.* **9**, 190–194.)